Structural study of C_2Cl_6 by Molecular Dynamics

Andrés Henao Aristizábal.
Supervisors: Elvira Guardia, Luis Carlos Pardo.

Departament de Fisica i Enginyeria Nuclear, Universitat Politecnica de Catalunya, Barcelona.

Abstract

A Molecular Dynamics study of hexachloroethane C_2Cl_6 was done in order to study the structure at different temperatures, varying from 300K to 480K. The system at 480K showed a liquid phase, as reported in the literature. A comparison with an experimental neutron scattering structure factor was made obtaining good agreement. A simulated annealing was carried out in a range of 300 to 480K. The radial distribution functions were compared studying the thermal dependence of the structure, the mean square displacements and self diffusion coefficients were also analyzed to complete an image of the structural changes. The transition to the liquid phase is observed above 450K, this is in agreement with the reported melting temperature for this system of 458K.

Keywords: hexachloroethane, structure factor, radial distribution functions, molecular dynamics.

I. INTRODUCTION

Molecular dynamics simulations have been used for the study of condensed-phases since long time ago [1], [2]. These studies are not only able to characterize the structure and static properties of systems at the molecular level, but to describe the dynamical processes that undergo in these systems. Hexachloroethane (C_2Cl_6), is an interesting material with three different solid phases [3], [4] (orthorombic between 4 and 318K, monoclinic between 318 and 344K and a plastic phase stable from 344K up to the melting temperature $T_m = 458K$ [5]). In this study we will investigate the structural properties of the C_2Cl_6 liquid phase at 480K and the solid region in the range of temperatures between 300 and 450K. We will use classical molecular dynamics simulations to study radial distribution functions, structure factors, mean square displacements and self diffusion coefficients.

This work is divided as follows, Section II. explains the details of the force field, the molecular model employed and the simulation procedure. Section III. shows the results and discussion of static and structural properties, divided in subsections A. for the liquid phase at 480 K and subsection B. with the same properties for the simulated annealing starting from a solid structure at 300 K. Section IV. is devoted to analyze the mean square displacement and diffusion coefficients in all the range of temperatures simulated, comparing and relating them to the results of the Section III. Section V. is devoted to the concluding remarks and future work possibilities.

II. MOLECULAR MODEL AND COMPUTATIONAL DETAILS

The Gromos53a6 force field [6] was used, where the description of the system energy results from the sum of intramolecular interactions (bond stretching $U_{strecht}$, angle bending U_{bend}, dihedral torsion $U_{torsion}$) and intermolecular interactions that come from Van der Waals (Lennard-Jones U_{LJ}) and electrostatic (Coulomb $U_{coulomb}$) terms:

$$U = U_{strecht} + U_{bend} + U_{torsion} + U_{LJ} + U_{coulomb} \quad (1)$$

where the functional forms of these potentials are:

$$U_{strecht} = \sum_{n=1}^{N} \frac{1}{4} K_{b_n} \left[b^2 - b_0^2 \right]^2 \quad (2)$$

$$U_{bend} = \sum_{n=1}^{N} \frac{1}{2} K_{\theta_n} \left[\cos\theta - \cos\theta_0 \right]^2 \quad (3)$$

$$U_{torsion} = \sum_{n=1}^{N} K_{\phi_n} \left[1 + \cos(m_n \phi_n) \right] \quad (4)$$

$$U_{LJ} = \sum_{pairs\ i,j} \left(\frac{C_{12_{ij}}}{r_{ij}^{12}} - \frac{C_{6_{ij}}}{r_{ij}^{6}} \right) \quad (5)$$

$$U_{coulomb} = \sum_{pairs\ i,j} \frac{q_i q_j}{4\pi\epsilon_0} \frac{1}{r_i r_j} \quad (6)$$

Force field parameters [7] are given in Table I. A geometric view of the initial configuration of the molecule is shown in figure 1.

Molecular dynamic simulations were performed using the GROMACS 4.5.3 package [8], [9] with the following conditions: The simulations were carried out in the NPT ensemble. Velocities were generated according to a Boltzmann distribution at $T_{env} = 300K$, the V-rescale thermostat [10] was used to drive the temperature to $T = 480K$ and the Berendsen pressure coupling [11] kept $P = 1$ atm. The initial configuration was obtained by randomly disposing 128, 256 and 512 molecules in a cubic box with dimensions that set the initial density to $1000\ kg\ m^{-3}$. Standard periodic boundary conditions and the minimum image convention were applied. A cut off distance of 1.2 nm was used and corrections for Coulomb interactions beyond cut off were performed using the Particle Mesh Ewald [12], [13]. The switch method was used to bring from 0.6 to 0.7 nm the LJ potential to zero. After equilibration with the

steepest descent method to converge the maximum force to $100 \, \text{kJ} \, \text{mol}^{-1} \, \text{nm}^{-1}$ a trajectory of 0.5 ns was generated with a time step $\Delta t = 2 \, \text{fs}$.
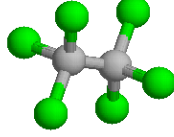

Fig. 1: Geometric view of the Hexachloroethane molecule, Carbons are gray and Chloride are green.

III. STATIC AND STRUCTURAL PROPERTIES

A. *Liquid Phase*

The results obtained in the liquid phase were compared between the different size system, yielding the same energies, slight differences in the density and equal radial distribution functions (rdf's) up to the half-box distance, it is for this reason that from now on we will only refer to the system of 512 molecules.
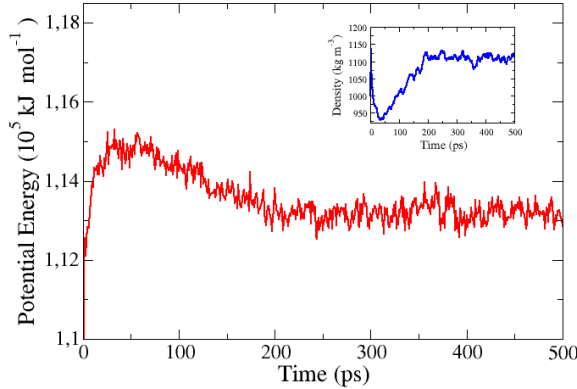

Fig. 2: Potential Energy as a function of the simulation time: (red line). The inset shows the density: (blue line)

Figure 2 shows the potential energy of the simulation, it finds an stable value after 200 ps and around the same time the simulation box fluctuates less than 1% and the density (as is shown in the inset of figure 2) stabilizes also. From now on we will take the last 200 ps to compute different equilibrium properties of the system, unless other is said. The average density of the simulated liquid phase is $1180 \, \text{kg} \, \text{m}^{-3}$.

The structure factor of the liquid phase of C_2Cl_6 can be characterized in terms of the atomic radial distribution functions $g_{\alpha\beta}(r)$, which gives the probabilities of finding atoms of type β at a distance r away from a center atom type α. In order to compare the simulation results with neutron scattering experiment, we construct the total radial distribution function [14]:

Table I. Force field parameters.

		Force Field	
	Atoms	b_0 nm	K_b kJ mol^{-1} nm^{-4}
Bonds	C-C	0.15730	2.7457 x 10^6
	C-Cl	0.17600	8.1000 x 10^6
	Atoms	θ_0 nm	K_θ kJ mol^{-1}
Angles	Cl-C-Cl	109.1	1440.0
	Cl-C-C	109.5	618.0
	Atoms	K_ϕ kJ mol^{-1}	multiplicity (m)
Dihedral	Cl-C-C-Cl	3.77	3
	Atoms	C_6 kJ mol^{-1} nm^6	C_{12} kJ mol^{-1} nm^{12}
NB LJ	C-C	2.3970816 x $x10^{-3}$	2.053489 x 10^{-4}
	C-Cl	4.5836352 x $x10^{-3}$	5.604463e x 10^{-5}
	Cl-Cl	8.7647044 x $x10^{-3}$	1.5295921 x 10^{-5}
	Atoms	C_6 kJ mol^{-1} nm^6	C_{12} kJ mol^{-1} nm^{12}
1-4 LJ	Cl-Cl	8.7647044 x 10^{-3}	1.5295921 x 10^{-5}

$$g_{total}(r) = g_{intra(r)} + g_{inter}(r) \qquad (7)$$

taking separetely the intra and inter molecular contributions:

$$g_{intra}(r) = \frac{b_C b_C g_{CC}(r) + 12 b_C b_{Cl} g_{CCl}(r) + 15 b_{Cl} b_{Cl} g_{ClCl}(r)}{W_{intra}} \qquad (8)$$

$$g_{inter}(r) = \frac{4 b_C b_C g_{CC}(r) + 24 b_C b_{Cl} g_{CCl}(r) + 36 b_{Cl} b_{Cl} g_{ClCl}(r)}{W_{inter}} \qquad (9)$$

where the numerical factors account for the number of possible pairs of two species and $b_C = 0.646$, $b_{Cl} = 0.9577$ are the neutron scattering lengths of the two atom types of our molecule. The weights are used to normalize the distributions:

$$W_{intra}(r) = b_C b_C + 12 b_C b_{Cl} + 15 b_{Cl} b_{Cl} \qquad (10)$$

$$W_{inter}(r) = 4 b_C b_C + 24 b_C b_{Cl} + 36 b_{Cl} b_{Cl} \qquad (11)$$

In figure 3 the computed C-C, C-Cl, Cl-Cl and total radial distribution functions are showed. The intra-molecular contributions are not presented here, as they are huge well defined peaks corresponding to the bond distances defined in the molecule model. The molecular coordination number n_c was computed for the first and second solvation shells, defined as the positions of the first and second minima of the total radial distribution function. In this case they are at $r_1 = 10.5$Å and $r_2 = 16.5$Å respectively:

$$n_{c_1} = 4\pi\rho \int_0^{r_1} r^2 g_{total}(r) dr \qquad (12)$$

$$n_{c_2} = 4\pi\rho \int_{r_1}^{r_2} r^2 g_{total}(r)dr \qquad (13)$$

For the first solvation shell it was found $n_{c_1} = 12.7$ molecules and $n_{c_2} = 39.43$ molecules for the second one.
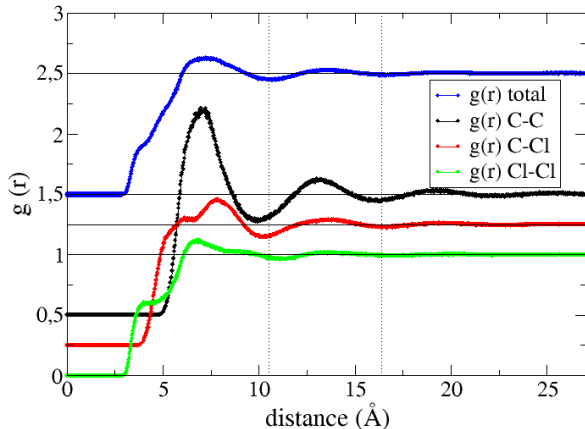

Fig. 3: Simulated partial and total radial distribution functions for $T = 480$K and $P = 1$ atm. The graphics are vertically displaced for clarity (0.25, 0.5, and 2.5 units), the horizontal line show the corresponding value for 1.

The neutron scattering structure factor was computed taking the Fourier transform of the total radial distribution function (see eq. 7):

$$S(q) - 1 = 4\pi\rho \int_0^{r_c} (g_{total}(r) - 1) \frac{\sin qr}{qr}dr \qquad (14)$$

We took the number density $\rho = 1$ and let it as a scaling factor to compare later with the experimental results. The cut off of the integration was taken as one of the last points of the radial distribution function intercepted by the 0 axis to avoid termination effects. Figure 4 shows the results of the neutron scattering experiment compared to the structure factor computed with eq. 14 for the simulation at the same conditions: $T = 480$K and $P = 1$ atm. Good agreement with the experiment is seen. The intermolecular structure contributes in the low q region, while the intramolecular contibutions are mostly important at large q values. Three well defined peaks appear at 1.0, 2.7 and 4.7 Å^{-1}.

B. Solid Phase and Simulated Annealing

After having obtained good agreement between the structure of the liquid phase between the simulation and the experimental results we study the evolution of the C_2Cl_6 starting from a solid phase at 300K and heating the system again up to 480K. Some changes in the simulation details presented in section II were made: The initial configuration was not constructed from random disposition since the sytem never reached the solid state, instead an initial BCC configuration was taken with molecules in the corners and
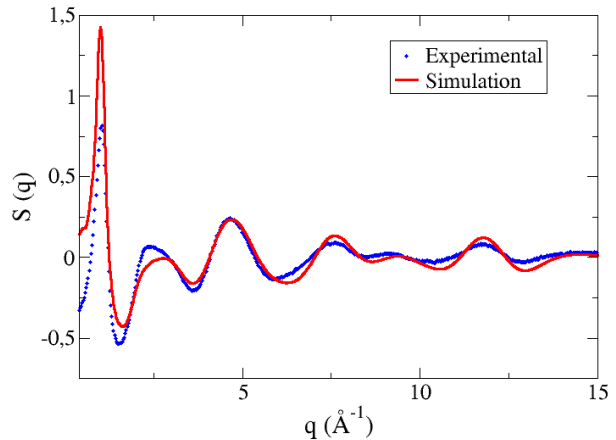

Fig. 4: Comparison between experimental: (blue dots) and MD simulation: (red line) structure factor. MD was performed at the same experimental conditions $T = 480$K and $P = 1$ atm

center of a unit cell, disposing in total 504 molecules. After initial equilibration with the steepest descent method velocities were generated at 150K and then we let the system evolve for 10 ps. After this a trajectory of 500 ps were generated. Starting from the final configuration at 300K we implemented a simulated annealing methodology to increase the temperature in 30K during 10 ps, and then equilibration of 100 ps for each temperature were allowed before heating again the system. By this way we obtained results at 7 different temperatures: 300, 330, 360, 390, 420, 450 and 480K. Densities are registered in Table II.

Table II. Densities as a function of the temperature.

Temperature (K)	Average density kgm^{-3}
300K	1680.0
330K	1656.5
360K	1610.7
390K	1581.3
420K	1530.9
450K	1371.1

Figure 5 shows the partial and total radial distribution functions at T=300K, the last one computed from eq. 7 We can see that important differences arise compared to the rdf's at 480K, strong oscillations with an slow decaying show the positional order of the system, as is expected for the solid phase temperatures registered for C_2Cl_6, between 4 and 344K [5].

The molecular coordination number was computed from eq. 12 and 13, defining the first and second solvation shells at 7.8Å, with $n_{c_1} = 8.2$ molecules, and 10.5Å, with $n_{c_2} = 4.22$ molecules respectively. Although the first solvation shell is not clearly defined as a minima in the total radial distribution

function, a change in the slope is observed besides the definition of the minima in the partial distributions. From here is clear a high ordered phase, consistent with the BCC initial structure.
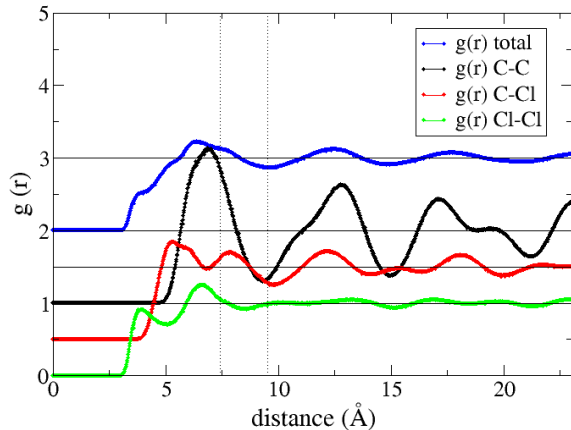

Fig. 5: Simulated partial and total radial distribution functions for $T = 300$K and $P = 1$ atm. The graphics are vertically displaced for clarity (0.5, 1.0 and 2.0 units), the horizontal lines show the corresponding value for 1.

Finally figure 6 show the temperature dependent evolution of the partial C-Cl radial distribution function, since it contains good qualitative structure arrangement of C_2Cl_6 and marked differences arise. The $g_{ccl}(r)$ is presented from bottom to top, with increasing temperature, displaced vertically and graphics at 330K and 390K are omitted for the sake of clarity, as they are intermediate to those presented. Three important features are present. The marked oscillations are damped from 450K. The first peak that is related to the distance at which the next neighbours start to locate changes in three stages, at 300K is well defined and from 360K it becomes wider beginning to decrease its high in comparison to the second peak to end being smaller at 480K. Finally the position of the second minima in $g_{ccl}(r)$, related to the first solvation shell, is displaced to the right as the temperature increases, which shows an expansion, as is given by the decrease of the density, and a possible change in the arrangement of first neighbours. It is interesting to see how at 420K occurs a change in the first two peaks, being a frontier where at lower temperatures the first peak is higher and the opposite happens when the temperature is above this point.

Figure 7 shows a molecule density map for the simulation box viewed from the z-axis for 300, 420, 450 and 480K, this density mapping is the average during 100 ps for each temperature. Red color indicates a higher density and therefore a higher localization of molecules. It is interesting to confirm the change that we observed mathematically in the radial distribution functions (figure 6) seeing a high ordering in figures 7a and 7b, lower molecule localization (premelting
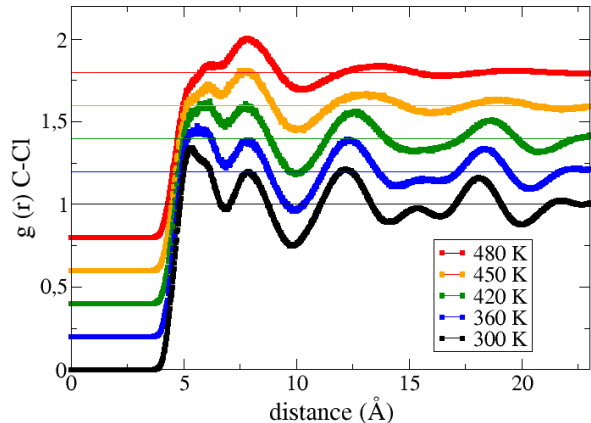

Fig. 6: Simulated Partial g_{C-Cl} Radial distribution functions for different temperatures and $P = 1$ atm, the graphics are vertically displaced for clarity (0.2 units each), the horizontal line shows the corresponding value for 1. From bottom to top: 300, 360, 420, 450 and 480 K.

effects) in figure 7c and a no localized state in figure 7d, corresponding to the liquid phase.

IV. MEAN SQUARE DISPLACEMENT

Analysis of the mean square displacement MSD as a function of the simulation time and for the different temperatures in the present work was made. The mean square displacement was computed for the equilibration time for each temperature (100 ps). The results are shown in figure 8. The MSD is presented from bottom to top in order of increasing temperature, MSD's at 330 and 390K are omitted as they are only intermediate between 300-360K and 360-420K respectively. The long time curve has a low slope, almost constant, up to 420K, this is a typical behaviour in a system with low diffusivity, the atoms are nearly in the same position. The behaviour changes at 450 and 480K, where the slope of the long time curve increases considerably, it is in this temperature region that the change to a liquid phase is expected ($T_m = 458$K). This results are in concordance with the change observed in the radial distribution functions at the same values of temperature.

The self diffusion coefficient was taken as the slope of the MSD between 5 ps and 50 ps according to the Einstein relation:

$$D = \frac{1}{6t} \lim_{t \to \infty} < [r(t_0 + t) - r(t_0)]^2 > \qquad (15)$$

Figure 9 shows the results of the self diffusion coefficients for different temperatures, as it was expected from the mean square displacement, the diffusivity is very low and almost constant up to 420K. At 450K the system starts to present the diffusion process; as is expected for a liquid phase, and the diffussion coefficient is higher at 480K. Again this
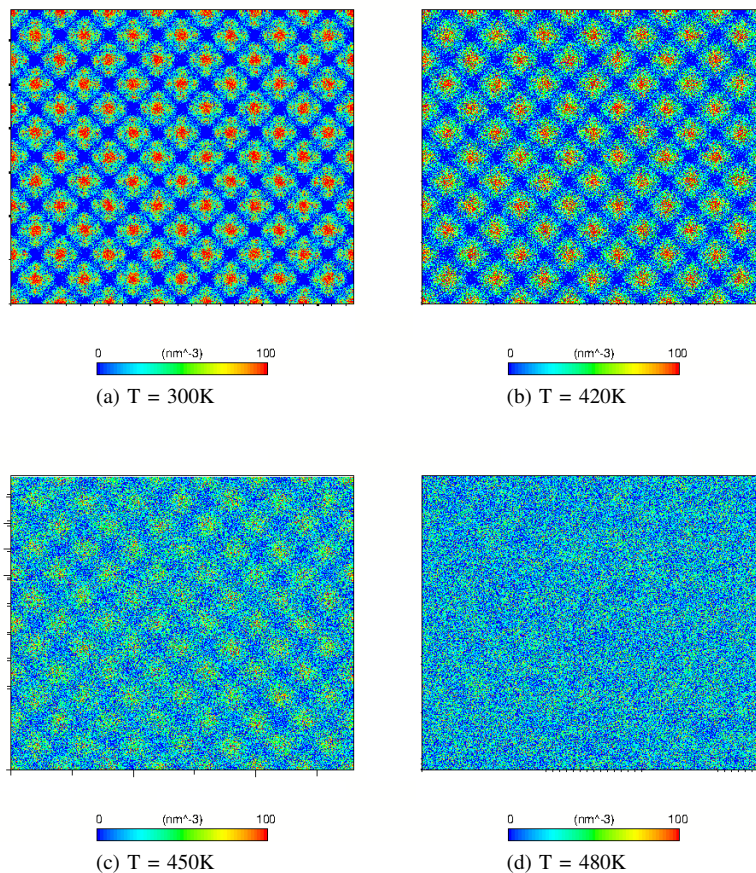
Fig. 7: Density map of molecules viewed from the Z-axis for the simulation box. Color scale indicates growing density mapping from blue to red.
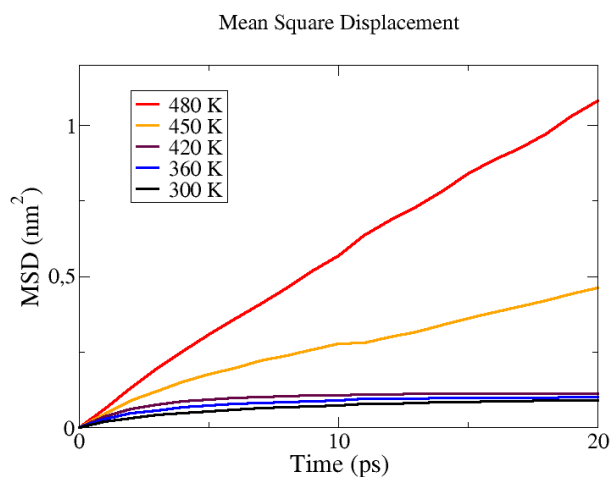

Fig. 8: Mean square displacement (for different system temperatures. From bottom to top: 300, 360, 420, 450 and 480 K.
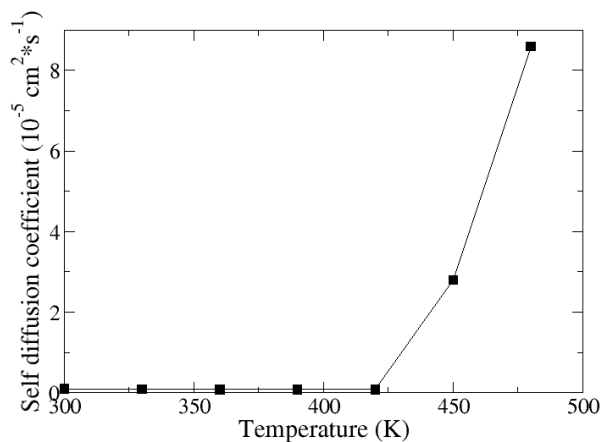

Fig. 9: Self diffusion coefficient as a function of the temperature.

result agrees with the mean square displacement and radial distribution function changes.

V. CONCLUDING REMARKS AND FUTURE WORK

Using classical molecular dynamics simulation we have studied structural properties for a liquid phase (480K) and

a solid region (300-450K) of C_2Cl_6. We have obtained good agreement between experimental neutron scattering and simulation structure factors in the liquid phase. The evolution of the partial radial distribution functions (g_{ccl} see figure 6) along the temperature showed the transition from solid (high ordered phase) to liquid phase, this transition occurred around 450K temperature, which is in agreement with the melting temperature of C_2Cl_6 $T_m = 458K$ considering that the simulation fluctuations were around 10K, this proved us the validity of the force field and the parameters taken to describe the C_2Cl_6 . Results of mean square displacements and self diffusion coefficients are in agreement with static properties, the C_2Cl_6 went from a low diffusivity region to a high diffusivity one begginning at 450K.
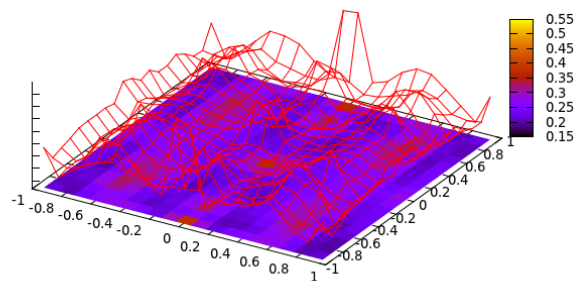
Further analysis should be carried out in the region of (300-450K) in order to study the orientational structure and dynamics, to identify the reported plastic phase [3], [4]. At the time we are studying the spatial distribution functions [15] defining vectorial and planar products to define the disposition and orientation of the molecules at different solvation shells to learn about the orientational changes, for this we use the results of the radial distribution functions and coordination numbers in order to analyze separately each solvation shell. Figure 10 shows some bivariate analysis; related to the spatial distributions, at room temperature and at the liquid phase at 480K. Analysis in the region (344-458K) will be conducted to gain knowledge of this system and about the orientational transition between plastic and liquid phases.

(a) T = 300K
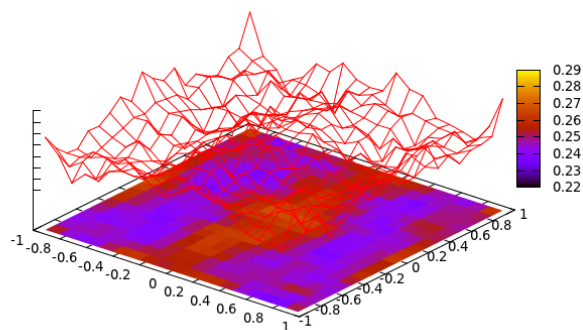

(b) T = 480K

Fig. 10: Spatial Distributions.

REFERENCES

[1] **Alder, B. J.; Wainwright, T.E.** *Studies in Molecular Dynamics. I. General Method.* **J. Chem. Phys.** 31, 459-466, **1959**.

[2] **Rahman, A.** *Correlations in the Motion of Atoms in Liquid Argon* **Phys. Rev.** 136 (2A), A405-A411, **1964**.

[3] **Criado, A.; Muñoz, A.** *A molecular dynamics simulation of the plastic phase of hexachloroethane.* **Molecular Physics.** 83, 815-833, **(1994)**.

[4] **Criado, A.; Muñoz, A.** *A molecular dynamics interpretation of the inelastic neutron spectra in the plastic phase of hexachloroethane.* **Molecular Physics.** 84, 1207-1225, **(1995)**.

[5] **Seki, S.; Momotani, B.** *Heats of Transition of Hexachloroethane.* **Bull. Chem. Soc. Jpn.** 23, 30-31, **(1950)**.

[6] **Oostenbrik, C.; Villa A.; Mark, A.E.; Van Gunsteren, W.F.** *A Biomolecular Force Field Based on the Free Enthalpy of Hydration and Solvation: The GROMOS Force-Field Parameter Sets 53A5 and 53A6.* **J. Comp. Chem.** 25, 1656-1676. **(2004)**.

[7] **Alpeshkumar, K.; Malde, A.K.; Le Zuo; Breeze, M.; Stroet, M; Poger, D.; Nair, P.C.; Oostenbrink, C.; Mar A.E**. Molecular Dynamics group, School of Chemistry and Molecular Biosciences (SCMB), The University of Queensland, QLD 4072, Australia. (http://compbio.biosci.uq.edu.au/atb).

[8] **Berendsen, H.J.C.; Van der Spoel, D.; van Drunen, R**. *GROMACS: A message-passing parallel molecular dynamics implementation.* **Computer Phys. Communications.** 91, 43-56, **(1995)**.

[9] **Hess, B.; Kutzner, C.; Van der Spoel, D.; Lindahl, E.** *GROMACS 4: Algorithms for Highly Efficient, Load-Balanced, and Scalable Molecular Simulation.* **J. Chem. Theory Comput.** 4, 435-447, **(2008)**.

[10] **Bussi, G.; Donadio, D.; Parrinello, M**. *Canonical sampling through velocity rescaling.* **J. Chem. Phys.** 126, 014101 **(2007).**

[11] **Berendsen, H.J.C.; Postma, J.P.M.; van Gunsteren, W.F.; DiNola, A.; Haak, J.R.** *Molecular dynamics with coupling to an external bath.* **J. Chem. Phys.** 81, 3684-3690, **(1984)**.

[12] **Darden, T.; York, D.; Pedersen, L.** *Particle mesh Ewald: An N*logN method for Ewald sums in large systems.* **J. Chem. Phys.** 98, 10089-10092, **(1993)**.

[13] **Essmann, U.; Perera, L.; Berkowitz, M.L.; Darden, T.; Lee, H.; Pedersen, L.G.** *A smooth particle mesh Ewald method.* **J. Chem. Phys.** 103, 8577-8593, **(1995)**.

[14] **Fischer, H.E; Barnes, A.C; Salmon, P.** *Neutron and x-ray diffraction studies of liquids and glasses.* **Rep. Prog. Phys.** 69, 233-299, **2006**.

[15] **Pardo L.C., Tamarit J.Ll., Veglio N., Bermejo F.J., and Cuello G.J.** *Comparison of short-range-order in liquid- and rotator-phase states of a simple molecular liquid: A reverse Monte Carlo and molecular dynamics analysis of neutron diffraction data.* **Phys. Rev. B.** 76, 134203 (2007)